

**Organic charge transfer complex at the boundary between superconductors
and insulators: the critical role of a marginal part of conduction pathways**

Toshio Naito,^{†,‡,*} Hayato Takeda,[†] Yusuke Matsuzawa,[†] Megumi Kurihara,[†] Akio Yamada,[†]
Yusuke Nakamura,[†] and Takashi Yamamoto^{†,‡,‡}

[†]Graduate School of Science and Engineering, Ehime University, Matsuyama 790-8577, Japan.

[‡]Geodynamics Research Center (GRC), Ehime University, Matsuyama 790-8577, Japan.

[‡]Research Unit for Development of Organic Superconductors, Ehime University, Matsuyama
790-8577, Japan.

*Corresponding author: tnaito@ehime-u.ac.jp

Contents

1.	Electrocrystallization conditions for κ -ET ₂ Cu[N(CN) ₂]I (1)	p. 2
2.	Single crystal X-ray structural analyses	p. 2
3.	Electrical resistivity measurements	p. 8
4.	Quantum chemistry calculations	p. 16
5.	Extended Hückel tight-binding band calculations	p. 16
5.	References	p. 18

§1. Electrocrystallization conditions for κ -ET₂Cu[N(CN)₂]I

Table S1. Typical electrocrystallization conditions for κ -ET₂Cu[N(CN)₂]I (**1**).^{*)}

ET (mg)	Na[N(CN) ₂] (mg)	CuI (mg)	18-crown-6 ether (mg)	CH ₂ Cl ₂ (mL)	Current Density (μ A·cm ⁻²)
10.3	11.4	22.6	40.0	10	5.0
12.1	10.9	23.5	43.4	15	2.5

^{*)} All the reagents were used as received except for pre-drying of 18-crown-6 under vacuum at room temperature and grinding of ET in agate mortar prior to use. Platinum wires (1 mm in diameter) were used as electrodes. N₂ atmosphere under 35°C.

§2. Single crystal X-ray structural analyses

As preliminary examination for selecting the single crystals suitable for the physical measurements in this work, the X-ray oscillation photographs were taken using a RIGAKU R-AXIS RAPID/R-XG1 (graphite monochromated Mo-K _{α} radiation; $\lambda = 0.71073$ Å) at 296 K. Single crystal X-ray structural diffraction was performed using a RIGAKU VariMax SaturnCCD724/ α (graphite monochromated Mo-K _{α} radiation; $\lambda = 0.71073$ Å) and a RIGAKU VariMax RAPID/ α (multi-layer mirror monochromated Cu-K _{α} radiation; $\lambda = 1.54187$ Å) equipped with a nitrogen gas flow temperature controller (Cobra, Oxford Cryosystems). Regarding the low-temperature measurements, the cooling rate was -1 K/min, which was the same with that of the resistivity measurements. When rapid cooling was required, the cooling rate was -100 K/min from 296 to 100 K. The fluctuation in temperature during the data collections was $\sim\pm 1$ K. The collected data were processed using CrysAlisPro ver. 171.38.46 or ver. 171.41_64.93a (Rigaku Oxford Diffraction) prior to the structure determination and refinement using CrystalStructure 4.3.2 or Olex 2-1.5 (Rigaku). The hydrogen atoms on the ordered ethylene groups of the ET molecules were located at the calculated positions. The hydrogen atoms on the disordered ethylene groups were neither found by the Fourier synthesis nor located at the calculated positions. The distances between the hydrogen and iodine atoms were estimated using the calculated positions of the H atoms for each conformation of the ethylene groups. Selected crystallographic data are shown in **Table S2**. Details of the analysis along with the crystallographic data have been deposited with Cambridge Crystallographic Data Centre.

Table S2. Selected crystal data of **1^{a)}**

Temperature (K)	296		
Sample # ($R(\%)$ ^{b)})	#2 (58(9))	#3 (53(5))	#5 (57(5))
Electrical behavior	IM	Ins	SC
a (Å)	12.9118(5)	12.9208(3)	12.9101(4)
b (Å)	30.3410(11)	30.2576(7)	30.2796(10)
c (Å)	8.6516(3)	8.6412(2)	8.6523(3)
V (Å ³)	3389.3(2)	3378.31(13)	3382.29(19)
D_{calc} (g cm ⁻³)	2.010	2.017	2.014
CCDC deposit #	2001305	2001310	2001312
Temperature (K)	100		
Sample # ($R(\%)$ ^{b)})	#1 (54(3))	#2 (60(2))	#3 (63(2))
Electrical behavior	Ins	IM	Ins
a (Å)	12.7066(5)	12.6951(3)	12.6806(3)
b (Å)	29.9277(10)	29.9226(5)	29.9198(5)
c (Å)	8.6211(3)	8.64092(16)	8.65985(16)
V (Å ³)	3278.4(2)	3282.43(11)	3285.56(11)
D_{calc} (g cm ⁻³)	2.078	2.076	2.074
CCDC deposit #	2126205	2001301	2001308
Temperature (K)	100		
Sample # ($R(\%)$ ^{b)})	#4 (73(3))	#5 (76(2))	—
Electrical behavior	IM	SC	—
a (Å)	12.6628(2)	12.6933(2)	—
b (Å)	30.0177(5)	30.0387(5)	—
c (Å)	8.68694(16)	8.67757(16)	—
V (Å ³)	3301.98(10)	3308.67(10)	—
D_{calc} (g cm ⁻³)	2.063	2.059	—
CCDC deposit #	2126206	2001311	—

^{a)} Formula: C₂₂H₁₆CuIN₃S₁₆, M (g mol⁻¹) = 1025.80, Crystal system: Orthorhombic, Space Group: *Pnma* (#62), $Z = 4$. ^{b)} The ratios of staggered conformation of the ethylene groups in ET at the given temperatures. In the low temperature X-ray single crystal structure analyses, the samples were slowly (−1 K/min) cooled down to 100 K. The data at 296 K for samples #1 and #4 are missing, because the crystals were broken or lost before the X-ray structural analyses at 296 K.

Table S2 (continued). Selected crystal data of **1^{a)}**

Temperature (K)	296		
Sample # (<i>R</i> (%) ^{b)})	#6 (52(2))	#7 (55(3))	#8 (56.8(16))
Electrical behavior	SC	IM	IM
<i>a</i> (Å)	12.8915(4)	12.8867(4)	12.8892(4)
<i>b</i> (Å)	30.2499(8)	30.2590(9)	30.2507(8)
<i>c</i> (Å)	8.6831(2)	8.6857(2)	8.6770(2)
<i>V</i> (Å ³)	3386.12(16)	3386.89(17)	3383.23(16)
<i>D</i> _{calc} (g cm ⁻³)	2.016	2.012	2.014
CCDC deposit #	2114421	2114420	2110351

^{a)} Formula: C₂₂H₁₆CuIN₃S₁₆, *M* (g mol⁻¹) = 1025.80, Crystal system: Orthorhombic, Space Group: *Pnma* (#62), *Z* = 4. ^{b)} The ratios of staggered conformation of the ethylene groups in ET at the given temperatures.

Table S2 (continued). Selected crystal data of **1^{a)}**

Temperature (K)	100		
Sample # (<i>R</i> (%) ^{c)})	#6 (73.2(10);72.3(11))	#7 (71(2);69.7(16))	#8 (68.1(12);72.6(10))
Electrical behavior	SC	IM	IM
<i>a</i> (Å) ^{c)}	12.6749(3);12.6697(3)	12.6844(5);12.6524(3)	12.6735(2);12.6853(2)
<i>b</i> (Å) ^{c)}	30.0135(6);29.9957(6)	29.9858(9);29.9686(7)	30.0068(5);30.0090(5)
<i>c</i> (Å) ^{c)}	8.7173(2);8.7154(2)	8.7084(3); 8.6953(2)	8.7181(1);8.7103(1)
<i>V</i> (Å ³) ^{c)}	3316.22(13);3312.17(13)	3312.3(2);3297.04(13)	3315.42(9);3315.78(9)
<i>D</i> _{calc} (g cm ⁻³) ^{c)}	2.057;2.057	2.057;2.067	2.055;2.055
CCDC deposit # ^{c)}	2114422;2110353	2110354;2110364	2110352;2110365

^{a)} Formula: C₂₂H₁₆CuIN₃S₁₆, *M* (g mol⁻¹) = 1025.80, Crystal system: Orthorhombic, Space Group: *Pnma* (#62), *Z* = 4. ^{b)} The ratios of staggered conformation of the ethylene groups in ET at the given temperatures. In the low temperature X-ray single crystal structure analyses, the samples were slowly (−1 K/min) cooled down to 100 K. ^{c)} The left and right numbers show the values in the slow (−1 K/min; left) and rapid (−10 K/min; right) cooling processes, respectively.

Table S3. Shortest interatomic distances between hydrogen atoms located at neighboring ET molecules (C-H...H) and those between hydrogen and halogen atoms in the anions (C-H...X) in selected superconducting and related ET salts. ^{a)}

Salts	C-H...H (Å)	C-H...X (Å)	Ref.
β -ET ₂ IBr ₂ (127 K)	2.17	2.89	S1
β -ET ₂ AuI ₂ (127 K)	2.22	2.97	S1
β -ET ₂ I ₃ (127 K)	2.15 ^{b)}	2.84 ^{c)}	S1
β^* -ET ₂ I ₃ (127 K)	2.16	3.01	S1
κ -ET ₂ Cu[N(CN) ₂]I (296 K)	2.205 ^{b)}	3.209 ^{c)}	This work
κ -ET ₂ Cu[N(CN) ₂]I (100 K, Rapid) ^{d)}	2.259 ^{b)}	3.317 ^{c)}	This work
κ -ET ₂ Cu[N(CN) ₂]I (100 K, Slow) ^{e)}	2.213 ^{b)}	3.066 ^{c)}	This work

^{a)} Note that the values for κ -ET₂Cu[N(CN)₂]I vary from crystal to crystal depending on the values of $R(\%)$. For another example, see the caption of Figure 3 in the main text. ^{b)} In the staggered ethylene groups ^{c)} In the eclipsed ethylene groups ^{d)} The sample was rapidly (-10 K/min) cooled from 296 K to 100 K. ^{e)} The sample was slowly (-1 K/min) cooled from 296 K to 100 K.

Table S4. Shortest interatomic distances involving hydrogen atoms in κ -ET₂Cu[N(CN)₂]X (X = Cl, Br, I). ^{a)}

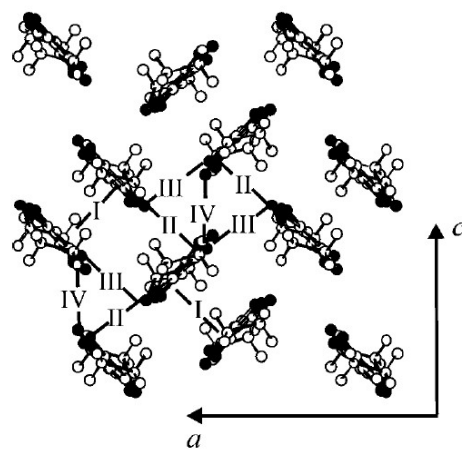
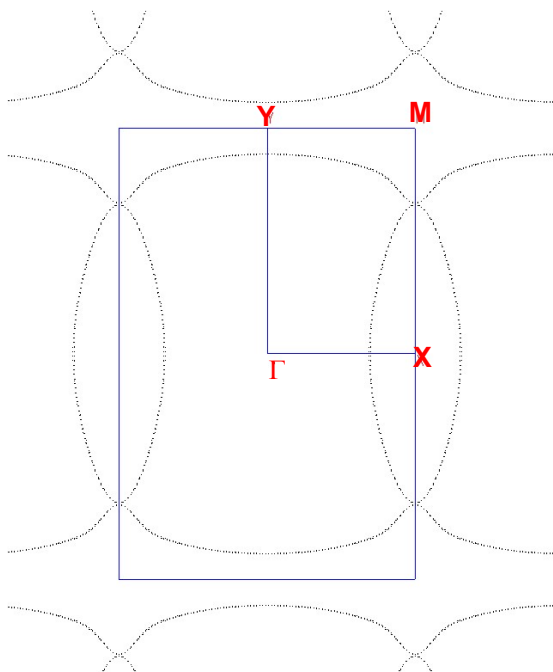
molecular pairs	bonding	X = Cl ^{b)}	X = Br ^{b)}	X = I ^{b)}	X = I ^{c)}	X = I ^{d)}	X = I ^{e)}
C-H...Donor	C-H...H	2.08	2.15	1.99 ^{f)}	2.160 ^{f)}	2.259 ^{f)}	2.213 ^{f)}
	C-H...S	2.77	2.77	2.58 ^{g)}	2.727 ^{g)}	2.823 ^{g)}	2.601 ^{g)}
C-H...Anion	C-H...N	2.66	2.69	2.55 ^{f)}	2.748 ^{f)}	2.602 ^{f)}	2.650 ^{f)}
	C-H...C	2.72	2.74	2.71	2.836 ^{h)}	2.790 ^{h)}	2.762 ^{h)}

^{a)} Note that the values for κ -ET₂Cu[N(CN)₂]I vary from crystal to crystal depending on the values of $R(\%)$. For another example, see the caption of Figure 3 in the main text. ^{b)} 127 K, Ref. [S1]. One of the two ethylene groups of each ET molecule in all three κ -ET₂Cu[N(CN)₂]X salts is disordered at 296 K. In the X = Cl and Br salts, the ethylene groups become ordered at 126 K, and the two ethylene groups of each ET molecule adopt an eclipsed conformation. ^{c)} 296 K. ^{d)} 100 K, the sample was rapidly (-10 K/min) cooled from 296 K to 100 K. ^{e)} 100 K, the sample was slowly (-1 K/min) cooled from 296 K to 100 K. ^{f)} Staggered arrangement. ^{g)} Eclipsed arrangement. ^{h)} The hydrogen belongs to the ordered ethylene groups.

Table S5. Calculated transfer energies (I–IV) for the single crystals with different lattice parameters for κ -ET₂Cu[N(CN)₂]I (**1**) and related salts.^{a)}

Salts	1		1		1	
Ser. #	9		10		11	
Properties b)	Ins		IM		SC	
<i>T</i> (K)	298	100	296	100	296	100
<i>a</i> (Å)	12.9614(2)	12.8361(2)	12.8805(17)	12.700(2)	12.9205(2)	12.6671(2)
<i>b</i> (Å)	30.0409(5)	29.7459(5)	30.301(5)	30.035(6)	30.3298(6)	29.9929(5)
<i>c</i> (Å)	8.51446(15)	8.46260(15)	8.6556(11)	8.6647(15)	8.66883(16)	8.68524(16)
<i>V</i> (Å ³)	3315.29(10)	3231.20(10)	3378.2(8)	3305.0(10)	3397.11(11)	3299.72(10)
I (eV)	0.4387	0.4540	0.4062	0.4120	0.3979	0.4296
II (eV)	0.1923	0.2079	0.1990	0.2213	0.1946	0.2265
III (eV)	0.0552	0.0507	0.0501	0.0385	0.0507	0.0345
IV (eV)	0.1254	0.1302	0.1112	0.0994	0.1048	0.0922
Salts	Br ^{c)}		Cl ^{d)}			
Ser. #	12		13			
Properties b)	SC		Ins			
<i>T</i> (K)	296	100	296	90		
<i>a</i> (Å)	12.961(3)	12.8369(3)	12.967(3)	12.898(3)		
<i>b</i> (Å)	29.996(7)	29.7581(6)	29.913(6)	29.53(2)		
<i>c</i> (Å)	8.5433(18)	8.45456(16)	8.4708(13)	8.395(7)		
<i>V</i> (Å ³)	3321.4(13)	3241.12(11)	3285.7(10)	3198(1)		
I (eV)	0.4243	0.4314	0.4521	0.4700		
II (eV)	0.1913	0.2138	0.1904	0.2066		
III (eV)	0.0548	0.0490	0.0581	0.0540		
IV (eV)	0.1211	0.1297	0.1294	0.1411		

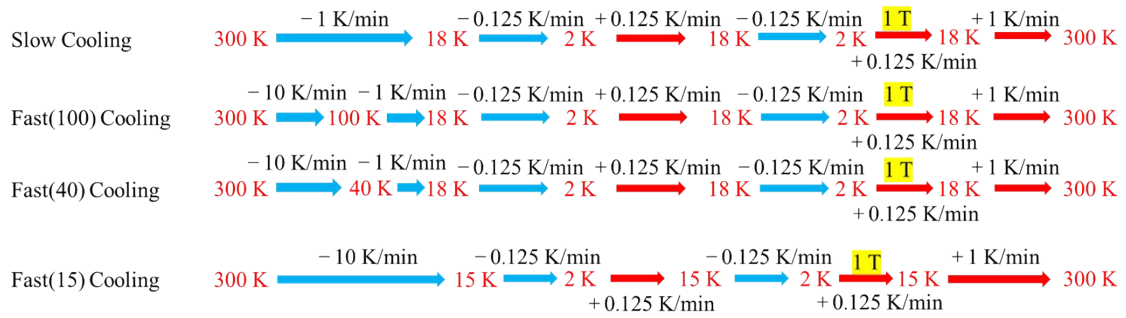
^{a)} In the case of salts containing disordered ethylene groups, the transfer energies were calculated by assuming that all the ethylene groups take either of the staggered or eclipsed conformations. As a result, both conformations gave identical calculation results to each other. For the intermolecular interactions I–IV and the resultant typical Fermi surfaces, see the figures below. ^{b)} Electrical behavior at the ground state and under ambient pressure. ^{c)} κ -ET₂Cu[N(CN)₂]Br (this work). ^{d)} κ -ET₂Cu[N(CN)₂]Cl (this work).



(Left) Fermi surfaces obtained from the transfer integrals #12 (100 K) in **Table S5**. All other sets of transfer integrals gave identical results with this figure. (Right) Donor arrangement shared by the salts in **Table S5** with labelling of the interactions.

§3. Electrical resistivity measurements

The single crystals of **1** having good crystal quality were selected based on the X-ray oscillation photographs taken prior to the resistivity measurements. They are usually square plates with the most developed dimension along the *a*-axis as the longest diagonal in the square (= the conducting *ac*-) plane. After cutting them in several pieces, the pieces having the dimension of ~ 1.0 mm along the *a*-axis were selected for the resistivity measurements. A standard four-probe method was used with gold wires (15 μm in diameter, Nilaco), gold paint (Tokuriki, No. 8560), and a Physical Property Measurement System PPMS-9 with an EverCool II (Quantum Design). The direct current of 100–200 μA was applied along the *a*-axis. Different cooling processes were examined for the same crystals as shown in Scheme S1. When the magnetic field dependence of resistivity was examined, the field of 1 T was applied in the normal direction of the conduction (*ac*-) plane during the heating process from 2 to 18 K.



Scheme S1. Different cooling processes examined in this study.

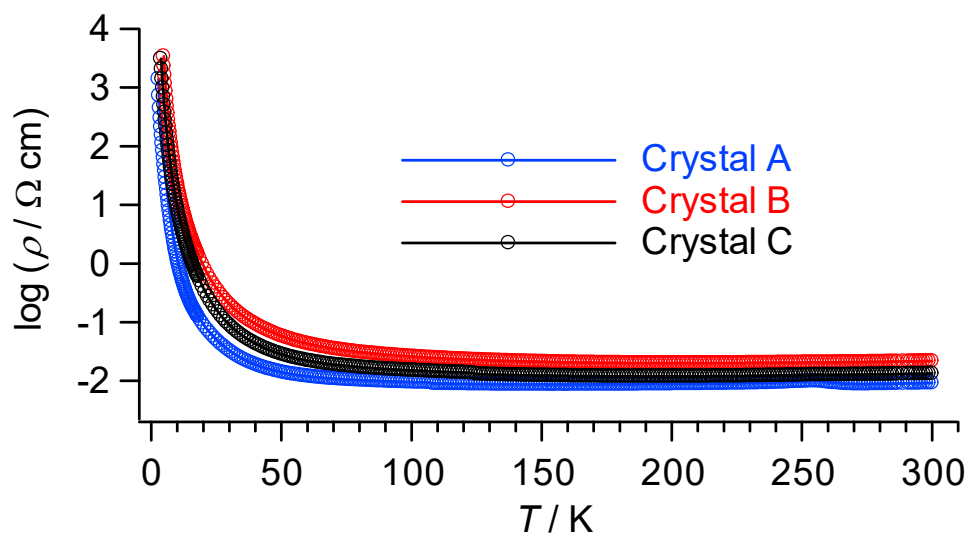


Figure S1. Electrical behavior of three pieces of crystals (A–C) originating from the same single crystal (#1; $R = 54(3)\%$ at 100 K). Only the data during the cooling process (-1 K/min) are shown. The heating data is identical in each crystal in the given scale of the plot above.

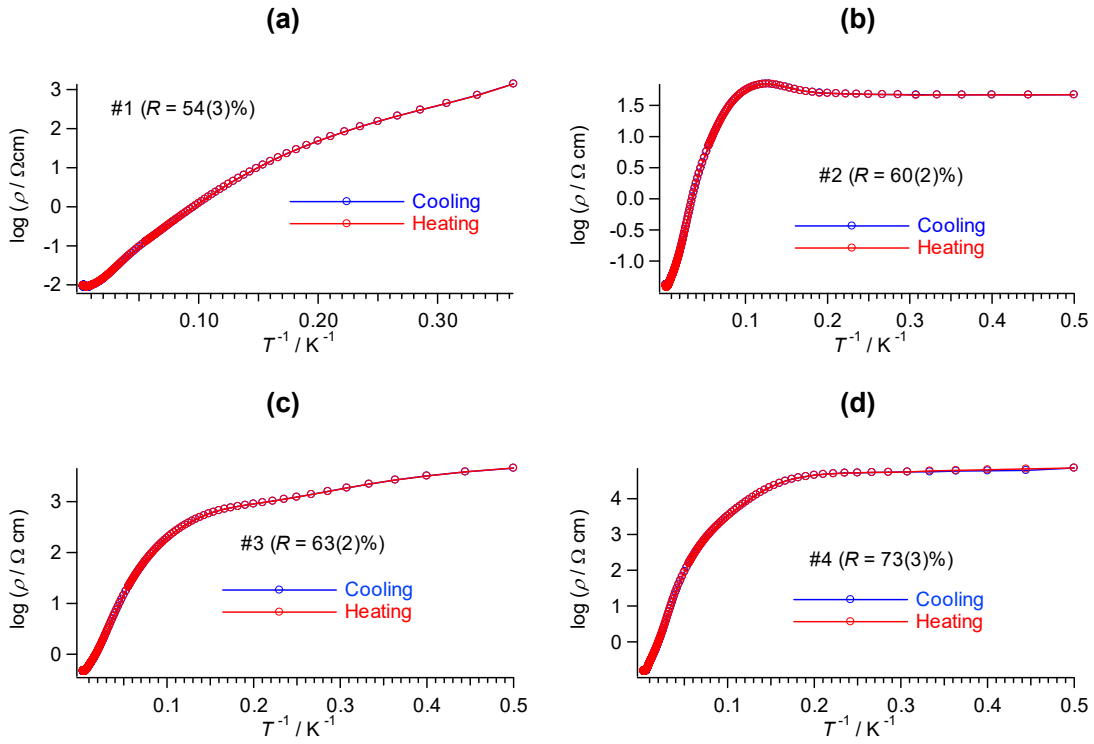


Figure S2. Arrhenius plots of the temperature-dependent resistivity (2–300 K). The cooling/heating rates were ± 1 K. The data during cooling and heating processes are completely overlapped in this scale. **(a)** Sample #1 ($R = 54(3)\%$), **(b)** Sample #2 ($R = 60(2)\%$), **(c)** Sample #3 ($R = 63(2)\%$), and **(d)** Sample #4 ($R = 73(3)\%$). The band insulators generally exhibit Arrhenius-type thermally activated behavior, where the electrical resistivity exponentially increases with the inverse of temperature. However, this is not the case with #1–#4.

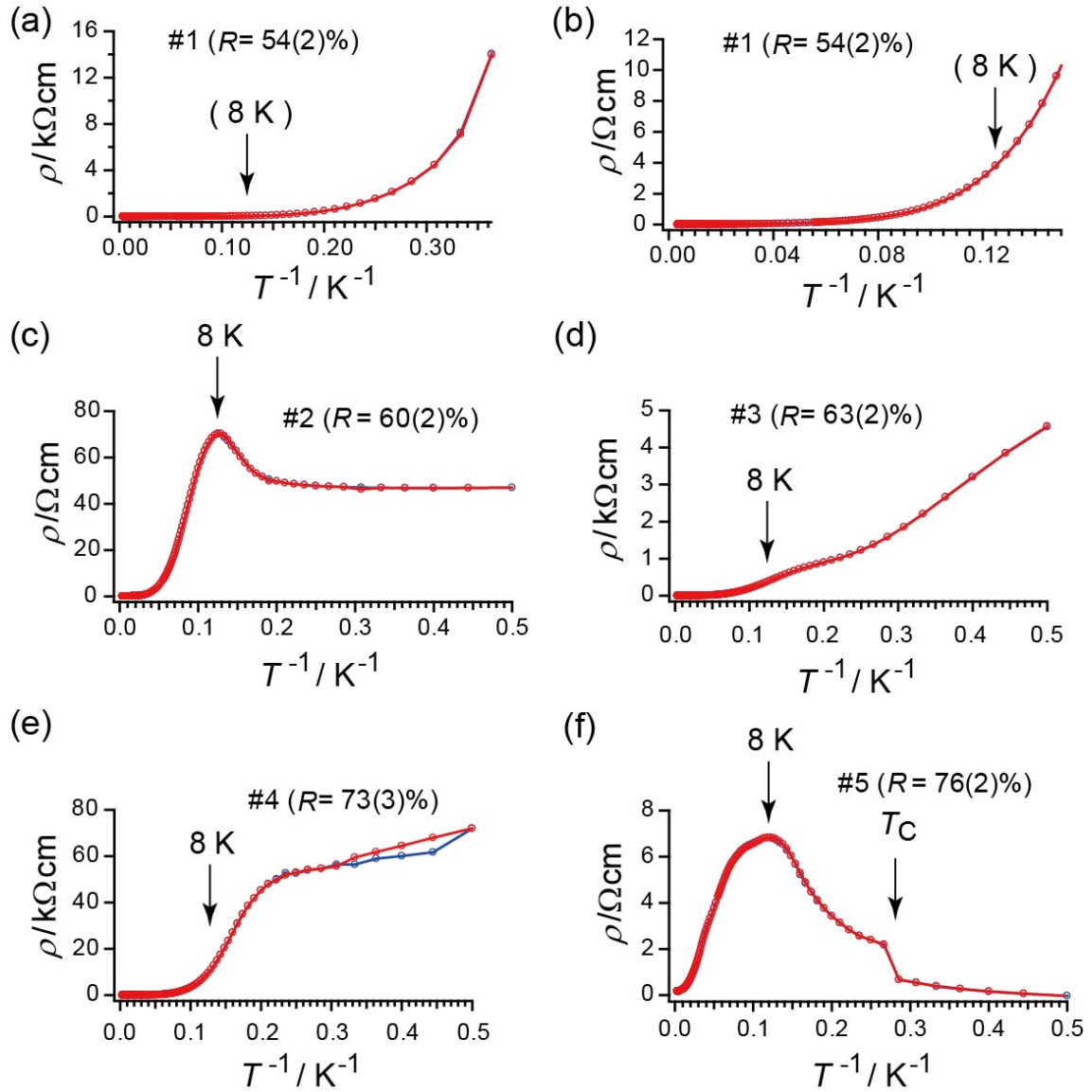


Figure S3. Resistivity vs. inverse of temperature. The same data with those in Figure 2 with different plots. **(a)** Sample #1, **(b)** enlarged view of Figure S3(a), **(c)** Sample #2, **(d)** Sample #3, **(e)** Sample #4, and **(f)** Sample #5. All the samples with SC or IM behavior exhibited maxima or inflection points at 8 K in the temperature dependence of resistivity. Both data during the cooling (blue) and heating (red) processes completely overlapped except for those in Figure S3(e).

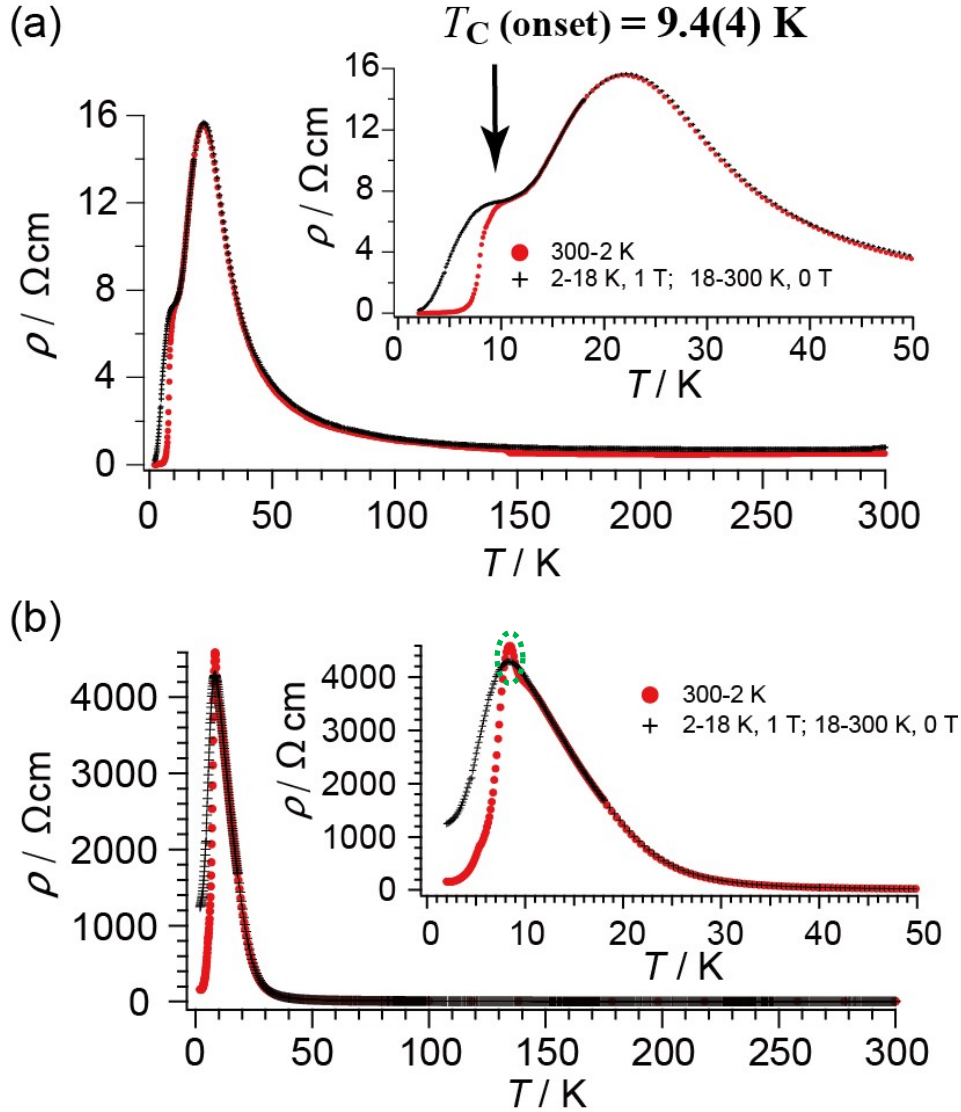


Figure S4. Various types of electrical behaviour observed for **1**. **(a)** A crystal (#6; $R = 73.2(10)\%$ at 100 K when slowly cooled (-1 K/min) down to 100 K) exhibiting an SC transition under the slow cooling process (-1 K/min ; “Slow Cooling” in Scheme S1). **(b)** A crystal (#7; $R = 69.7(16)\%$ at 100 K when rapidly cooled (-10 K/min) down to 100 K) exhibiting a broad SC transition under the rapid cooling process (-10 K/min ; “Fast(100) Cooling” in Scheme S1). ● Data acquired during a slow cooling (-1 K/min) process without applying magnetic field, + data acquired during a heating process from 2 to 300 K with applying magnetic field of 1 T between 2 and 18 K. The broken green oval in Figure S4(b) at $\sim 8\text{--}9 \text{ K}$ indicates negative magnetoresistance.

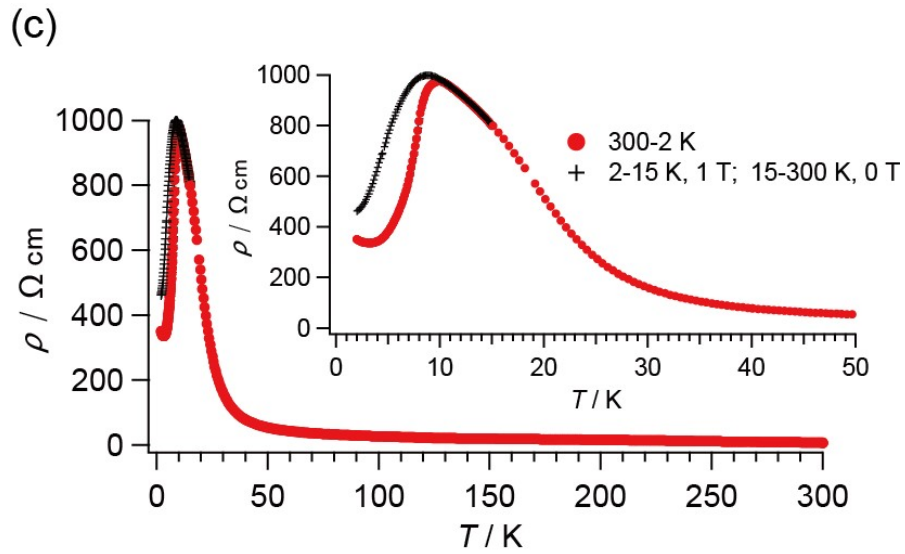


Figure S4 (Continued). Various types of electrical behaviour observed for **1**. (c) A crystal (#8; $R = 72.6(10)\%$ at 100 K when rapidly cooled (-10 K/min) down to 100 K) exhibiting intermediate or mixed behaviour between superconductors and insulators under the fast cooling process down to 15 K (-10 K/min ; “Fast(15) Cooling” in Scheme S1). The data in the warming process (15–300 K) are completely overlapped with those in the cooling process (300–15 K).

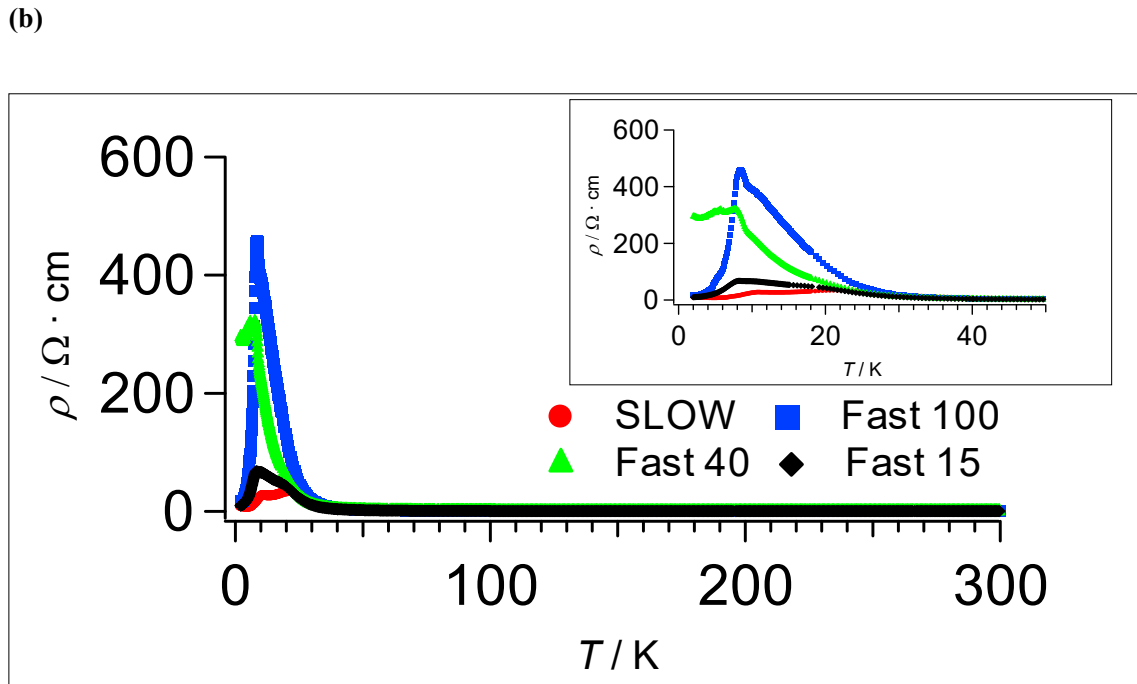
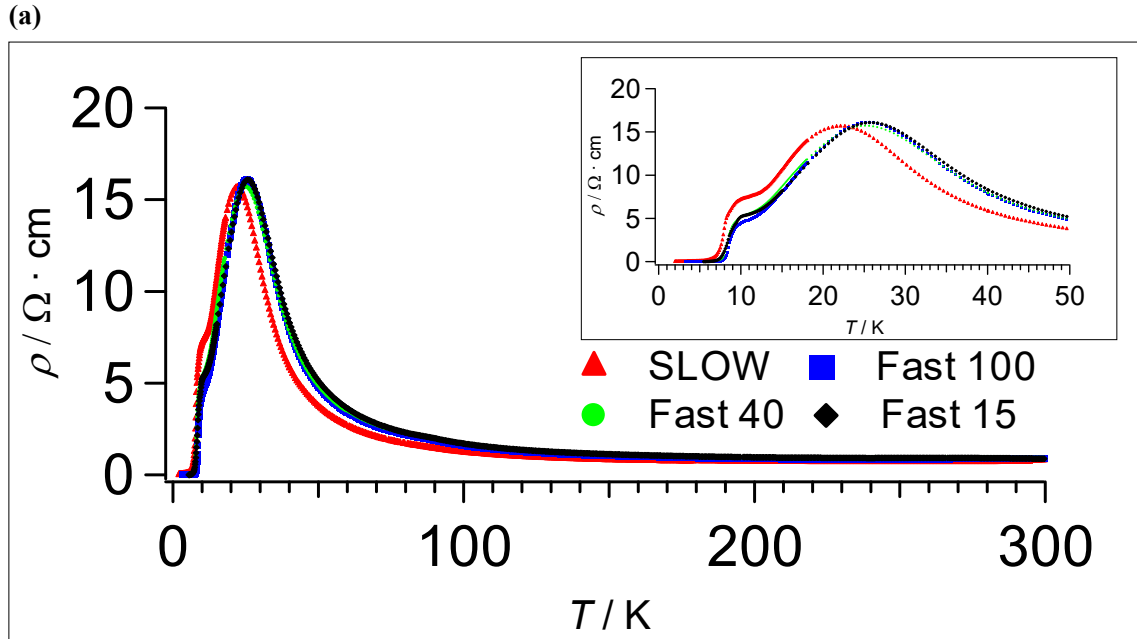


Figure S5. Dependence of electrical behaviour observed for **1** on the cooling processes. **(a)** A crystal (#6; $R = 73.2(10)\%$ at 100 K when slowly cooled (-1 K/min) down to 100 K) exhibiting SC transitions under different cooling processes (The same crystal as shown in Figure S4(a)). **(b)** A crystal (#7; $R = 69.7(16)\%$ at 100 K when rapidly cooled (-10 K/min)) exhibiting broad SC transitions under different cooling processes (Slow, Fast(100), Fast(40), and Fast(15)) except for the cooling process of “Fast 40” (The same crystal as shown in Figure S4(b)).

(c)

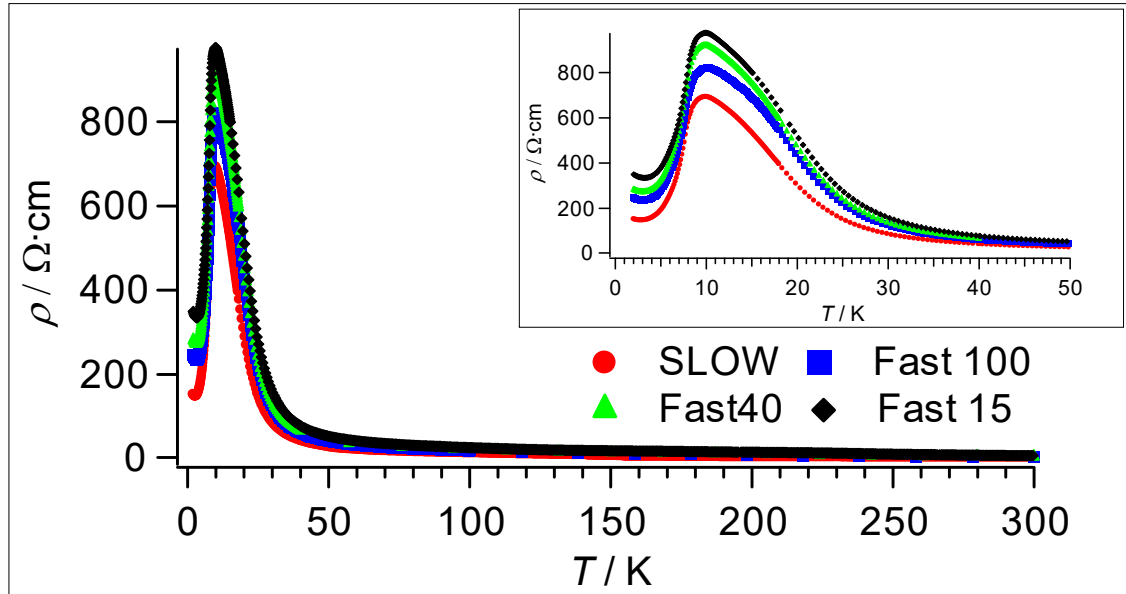


Figure S5 (Continued). Dependence of electrical behaviour observed for **1** on the cooling processes.

(c) A crystal (#8; $R = 72.6(10)\%$ at 100 K when rapidly cooled (-10 K/min) down to 100 K) exhibiting intermediate or mixed behaviour between superconductors and insulators (The same crystal as shown in Figure S4(c)).

Table S6. Temperature- and cooling-rate-dependences of R (%) for selected crystals.

Crystal #	R (296 K)	R (100 K; Slow)	R (100 K; Fast)
6	52(2)%	73.2(10)%	72.3(11)%
7	55(3)%	71(2)%	69.7(16)%
8	56.8(16)%	68.1(12)%	72.6(10)%

§4. Quantum chemistry calculations

Based on the atomic parameters of staggered and eclipsed forms of ET molecules obtained from the X-ray structural analysis of **1** at 100 K, a quantum chemistry calculation was carried out using Gaussian 09 (B3LYP/DGDZVP) and GaussView.^{S2,S3} The DFT calculation using B3LYP/3-21G gave nearly identical results, $\Delta E = \text{eclipsed} - \text{staggered} = 0.81 \text{ eV (3-21G) vs. } 0.91 \text{ eV (DGDZVP)}$, suggesting that the estimation is independent of basis functions within a framework of B3LYP. The model structures for the calculation were the following four types; (i) an isolated neutral ET molecule, (ii) an isolated monocation radical ET molecule, (iii) the same isolated neutral ET molecule with an anion $[\text{Cu}(\text{NC})(\text{NCN})\text{I}]^-$ beside ET, and (iv) the same isolated monocation radical ET molecule with an isolated anion $[\text{Cu}(\text{NC})(\text{NCN})\text{I}]^-$ beside ET. In the ET molecule in each model, both staggered and eclipsed conformations were examined. The structures (atomic parameters) of the ET and anion were taken from the results of X-ray structural analyses in this work as briefly shown in the table and structure optimization was not carried out. The energy difference ΔE between the two conformations were practically unchanged whether the cation-anion interaction (the hydrogen bonds) was considered or not in the 3-21G calculation, while ΔE was substantially changed ($+0.91 \text{ eV} \rightarrow -5.1 \text{ eV}$) in the DGDZVP calculation. ΔE was not affected whether the ET molecules were assumed to be neutral or a monocation radical as long as both conformations for comparison were assumed to have the same charges and the same chemical environment (whether the anion coexist or not).

§5. Extended Hückel tight-binding band calculations

Using the atomic parameters obtained from the X-ray structural analysis of **1**, the molecular orbital calculation was carried out based on an extended Hückel approximation using a free program package Caesar (vers. 1.0 & 2.0, PrimeColor Software). All the atoms of cations and anions of **1** are taken into consideration in order to check if there is any cation-anion interaction, i.e. band mixing. The parameters of atomic orbitals used in the calculation are tabulated in **Table S7**.

Table S7. H_{ii} and ζ used in band calculation.^a

atom	atomic orbital	H_{ii} (eV)	ζ_1	coeff. 1 ^b	ζ_2	coeff. 2 ^b
I	5s	-18.00	2.679	1.0000		
	5p	-12.70	2.322	1.0000		
	4s	-11.40	2.200	1.0000		
Cu	4p	-6.060	2.200	1.0000		
	3d	-14.00	5.950	0.5933	2.30	0.5744
S	3s	-20.00	2.662	0.5564	1.688	0.4873
	3p	-13.30	2.338	0.5212	1.333	0.5443
C	2s	-21.40	1.831	0.7616	1.153	0.2630
	2p	-11.40	2.730	0.2595	1.257	0.8025
N	2s	-26.00	1.950	1.0000		
	2p	-13.40	1.950	1.0000		
H	1s	-13.60	1.300	1.0000		

^a $H_{ii} = -\text{VSIP}$ (valence-state ionization potential [eV]). The double-zeta (for Cu 3d, S 3s, S 3p, C 2s, and C 2p) or single-zeta (for the remaining orbitals) Slater type orbitals (STO's) were used.

$$\chi_{\mu}(r, \theta, \phi) \propto r^{n-1} \exp(-\zeta r) Y(\theta, \phi) \text{ (single-zeta STO)}$$

$$\chi_{\mu}(r, \theta, \phi) \propto r^{n-1} [c_1 \exp(-\zeta_1 r) + c_2 \exp(-\zeta_2 r)] Y(\theta, \phi)$$

(double-zeta STO)

^b coeff. 1 and coeff. 2 correspond to 1 and 0 in single-zeta STO, and c_1 and c_2 in double-zeta STO, respectively.

§6. References

- (S1) Williams, J.M.; Schultz, A.J.; Geiser, U.; Carlson, K.D.; Kini, A.M.; Wang, H.H.; Kwok, W.-K.; Whangbo, M.-H.; Schirber, J.E. *Science* **1991**, *252*, 1501–1508.
- (S2) Gaussian 09, Revision C.01, Frisch, M. J.; Trucks, G. W.; Schlegel, H. B.; Scuseria, G. E.; Robb, M. A.; Cheeseman, J. R.; Scalmani, G.; Barone, V.; Mennucci, B.; Petersson, G. A.; Nakatsuji, H.; Caricato, M.; Li, X.; Hratchian, H. P.; Izmaylov, A. F.; Bloino, J.; Zheng, G.; Sonnenberg, J. L.; Hada, M.; Ehara, M.; Toyota, K.; Fukuda, R.; Hasegawa, J.; Ishida, M.; Nakajima, T.; Honda, Y.; Kitao, O.; Nakai, H.; Vreven, T.; Montgomery, J. A., Jr.; Peralta, J. E.; Ogliaro, F.; Bearpark, M.; Heyd, J. J.; Brothers, E.; Kudin, K. N.; Staroverov, V. N.; Kobayashi, R.; Normand, J.; Raghavachari, K.; Rendell, A.; Burant, J. C.; Iyengar, S. S.; Tomasi, J.; Cossi, M.; Rega, N.; Millam, J. M.; Klene, M.; Knox, J. E.; Cross, J. B.; Bakken, V.; Adamo, C.; Jaramillo, J.; Gomperts, R.; Stratmann, R. E.; Yazyev, O.; Austin, A. J.; Cammi, R.; Pomelli, C.; Ochterski, J. W.; Martin, R. L.; Morokuma, K.; Zakrzewski, V. G.; Voth, P. Salvador, G. A.; Dannenberg, J. J.; Dapprich, S.; Daniels, A. D.; Farkas, O.; Foresman, J. B.; Ortiz, J. V.; Cioslowski, J.; Fox, D. J. Gaussian, Inc., Wallingford CT, 2009.
- (S3) GaussView, Version 5, R. Dennington, T. Keith, J. Millam, *Semichem Inc.*, Shawnee Mission KS, 2009.